

Photoinduced Elimination in 2,3-Dihydro-2-*tert*-butyl-3-benzyl-4(1*H*)-quinazolinone: Theoretical Calculations and Radical Trapping Using TEMPO Derivatives

Fanny Araceli Cabrera-Rivera,^a Claudia Ortíz-Nava,^a Jaime Escalante,^{*a} Julio M. Hernández-Pérez,^b Minh Huy Hô^a

^a Centro de Investigaciones Químicas, Universidad Autónoma del Estado de Morelos, Av. Universidad 1001, C. P. 62209 Cuernavaca, Morelos, México
Fax +52(777)3297000; E-Mail: jaime@ciq.uaem.mx

^b Facultad de Ciencias Químicas, Benemérita Universidad Autónoma de Puebla, 14 Sur y Av. San Claudio, Col. San Manuel, 72530 Puebla, México

Received: 30.12.2011; Accepted after revision: 10.02.2012

Abstract: Photochemical irradiation of 2,3-dihydro-2-*tert*-butyl-3-benzyl-4(1*H*)-quinazolinone produced 3-benzyl-4(3*H*)-quinazolinone through photoinduced elimination via a radical mechanism. The use of photochemical conditions such as chloroform and UV irradiation ($\lambda = 254$ nm) got the 3-benzyl-4(3*H*)-quinazolinone in a high yield. Some theoretical calculations were achieved to explain the mechanism and the presence of radical intermediates was confirmed by trapping with different 2,2,6,6-tetramethylpiperidine-1-oxyl (TEMPO) derivatives.

Key words: 2,3-dihydro-4(1*H*)-quinazolinones, mechanism, photochemical reaction, 2,2,6,6-tetramethylpiperidine 1-oxyl (TEMPO), AIM, MO analysis, density analysis

4-Quinazolinone derivatives are important building blocks of active molecules isolated from different natural sources.¹ Their principal derivatives are 2,3-dihydro-4(1*H*)-quinazolinones and 4(3*H*)-quinazolinones. These compounds possess a wide range of useful biological activities and interesting pharmacological properties,² and their syntheses have been well described in the literature.³

The use of photochemical irradiation in these compounds, however, has been less common, and only a few have been reported such as preparation of fused quinazolin-4-one derivatives, for example, luotonin A and related fused compounds through radical intermediates,⁴ photodecomposition of 8-chloro-6-(2-fluorophenyl)-1-methyl-4*H*-imidazo[1,5-*a*][1,4]benzodiazepine (Midazolam) to get a 4(3*H*)-quinazolinone derivative,⁵ and irradiation of 4-phenylquinazolin-2-ones in the presence of a hydrogen donor in order to get the reduced 3,4-dihydroquinazolin-

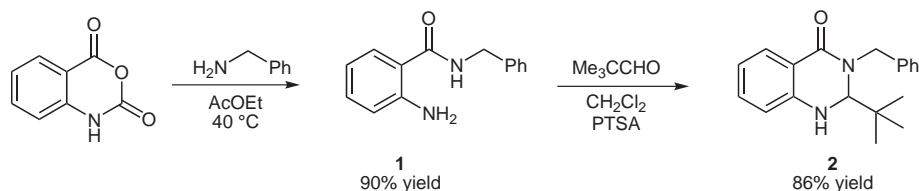
2-ones⁶ as well as the photoaddition of 4(3*H*)-quinazolinone derivatives to olefins.⁷

In this study we analyzed the behavior of 2,3-dihydro-2-*tert*-butyl-3-benzyl-4(1*H*)-quinazolinone under UV irradiation, and theoretical calculations were developed to propose a mechanism, and trapping of the radical intermediate was achieved using TEMPO derivatives. Knowledge of these reactions could help to develop photochemically controlled reactions of other 2,3-dihydro-4(1*H*)-quinazolinone derivatives.

Our research was focused on the preparation of starting materials following the methodology previously reported by our group⁸ in which a reaction between isatoic anhydride and benzylamine in ethyl acetate at 40 °C results in the corresponding aminobenzamide **1** in 90% yield. Next, the cyclocondensation of **1** with pivalaldehyde in dichloromethane and *p*-toluenesulfonic acid monohydrate gives **2** in 86% yield (Scheme 1).

Preliminary studies rapidly led to the conclusion that it was necessary to protect the reaction from light source since this would suffer photoinduced elimination and hence reduces the yield of compound **2**.

The absorption spectrum of **2** (Figure 1) presents two absorption bands at $\lambda = 242$ and 341 nm, attributed to $\pi-\pi^*$ and $n-\pi^*$ transitions, respectively. The fluorescence spectrum is shown in the Figure 2 and presents a maximum emission at $\lambda = 404$ nm. The quantum yield of fluorescence was measured at 25 °C using quinine sulfate (H_2SO_4 0.5 M, $\Phi = 0.55$) as standard and employing existing equations for calculating quantum fluorescence yield;



Scheme 1 Preparation of 2,3-dihydro-2-*tert*-butyl-3-benzyl-4(1*H*)-quinazolinone (**2**)

SYNLETT 2012, 23, 1057–1063

Advanced online publication: 29.03.2012

DOI: 10.1055/s-0031-1290492; Art ID: ST-2011-S0822-L

© Georg Thieme Verlag Stuttgart · New York

the quantum yield of **2** was 0.43. This implies that there might be other processes involved in addition to the fluorescence decay. On the other hand, for compound **2** we did not observe phosphorescence in solution at 25 °C.

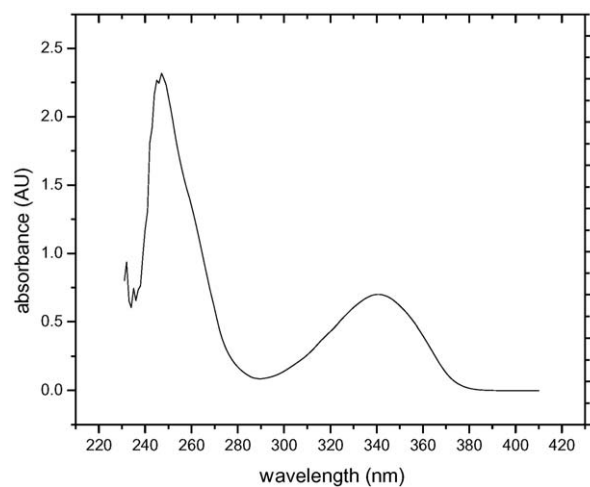


Figure 1 UV absorption spectrum, $2 \cdot 10^{-4}$ M in CHCl_3 at 25 °C

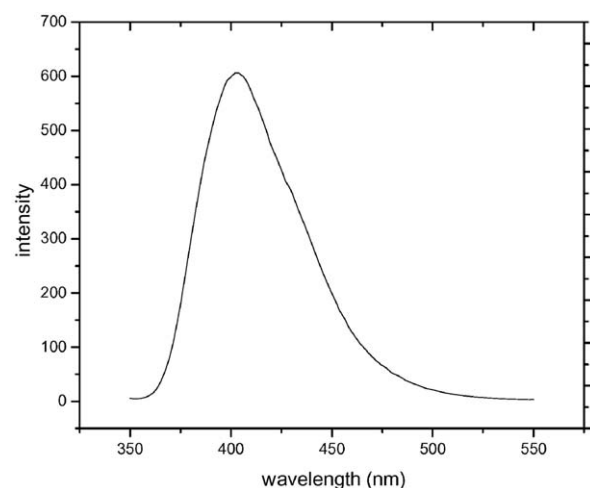
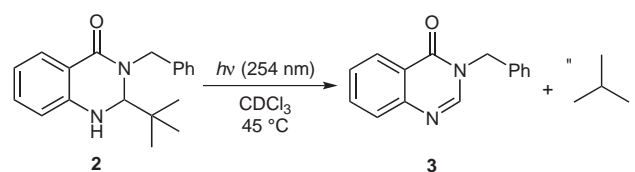


Figure 2 Fluorescence spectrum, $2 \cdot 10^{-6}$ M in CHCl_3 at 25 °C ($\lambda_{\text{ex}} = 336$ nm)

Coupling with the fact that the reaction may involve abstractions of either a hydrogen atom or a *tert*-butyl radical, we have decided to employ photochemical irradiation to facilitate radical cleavage. We first dissolved **2** in chloroform at room temperature, and then the compound underwent irradiation by means of UV light at $\lambda = 254$ nm. The result shows a mixture of starting material **2** and product **3**, which were further characterized by the partial 400 MHz ^1H NMR spectrum shown in Figure 3 (Table 1). Table 1 shows that this protocol permits better yield of product **3** under longer irradiation, close to 100% after 240 minutes.

The spectra of **2** following various irradiation durations are shown in Figure 3. Most notable here is the intensity of the signal H_d ($\delta = 5.16$ ppm) of the benzylic protons of

Table 1 Photochemical Irradiations of Compound **2**



Entry	Irradiation time (min)	Ratio 2/3
1	0	100:0
2	60	63:37
3	120	36:64
4	180	14:86
5	240	0:100

the product **3** as compared to the signals H_c and H_c' ($\delta = 3.92$ and 5.81 ppm, respectively) of the benzylic protons of **2**. One observes that H_c and H_c' are diminished with irradiation,^{8c,9} which finally disappeared after 240 minutes of irradiation.

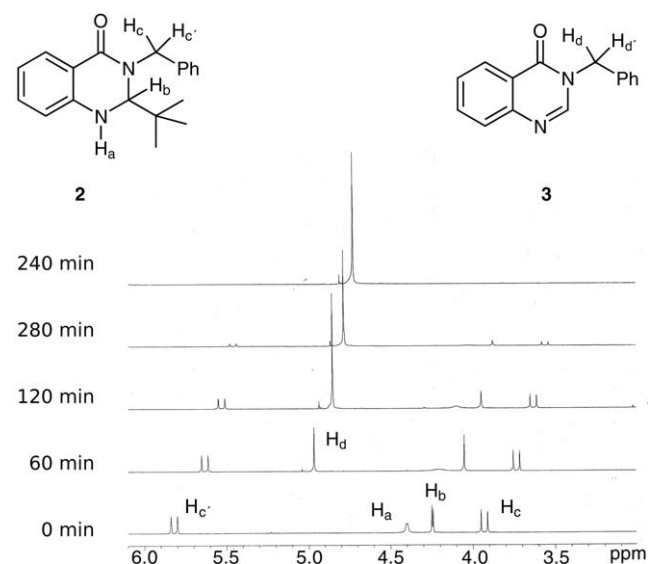
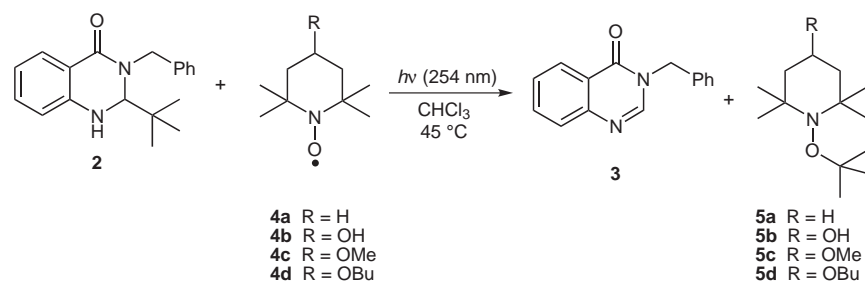


Figure 3 Partial 400MHz ^1H NMR spectra resulting from the irradiation of **2** with UV light ($\lambda = 254$ nm) in CDCl_3 at different reaction times

As shown below, the *tert*-butyl radical plays an important role in the mechanism, partially due to its well-known stability. We have decided to confirm the presence of this intermediate using TEMPO and derivatives.¹⁰

We employed 2,2,6,6-tetramethylpiperidine 1-oxyl (TEMPO) (**4a**), 4-hydroxy-TEMPO (TEMPOL, **4b**), 4-methoxy-TEMPO (**4c**), and 4-butoxy-TEMPO (**4d**). The results from Table 2 clearly show the corresponding *tert*-butyl derivatives **5a–d**.

It is important to note that the reaction times for entries in Table 2 were significantly longer than the time for the first

Table 2 Reaction of **2** with TEMPO Derivatives

Entry	TEMPO derivatives	Irradiation time (h)	Yield of 2 (%)	Yield of 3 (%)	Yield of 5 (%)
1	4a	25	31	63	5a 23
2	4b	25	17	81	5b 50
3	4c	25	33	64	5c 36
4	4d	25	0	95	5d 60

reaction showed in Table 1. This behavior could be explained by the variation in the rate constants of the trapping process, associated with the structure of the tertiary-centered carbon radicals in the presence of TEMPO derivatives, ranging from 10^9 to as low as 10^6 $\text{M}^{-1}\text{s}^{-1}$ for sterically hindered species.¹¹ For this reason, the reactions were carried out with different reaction times, but no significant change was detected. In our case, we have a system in which a dissociative mechanism would give rise to **2** in the presence of TEMPO derivative: re-association could then take place at either end. Inspection of the products shows that the *tert*-butyl radical has been trapped in moderate yield in all cases (Table 2). These results confirm the presence of the radical intermediate and support the idea that the mechanism occurs via free radicals.

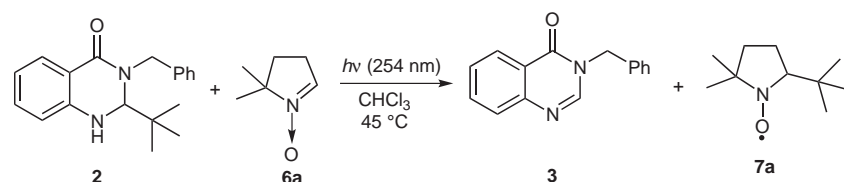
We have also applied a stronger thermal condition using a reflux system to 2,3-dihydro-2-*tert*-butyl-3-benzyl-4(1*H*)-quinazolinone in toluene and have not detected any elimination product after eight hours. It is suggested that the reaction is not thermodynamically driven.

Nitrones are a class of compounds, which are used as spin-trapping reagents, in particular DMPO [5,5-dimethyl-1-pyrroline-*N*-oxide (**6a**)] is one of the most commonly used. DMPO can spin trap superoxide, hydroxyl, and small carbon-centered free radicals, giving spin-trapped adducts with defined EPR spectra. We carried out an experiment using DMPO as radical scavenger. The result in

Table 3 shows only product **3** in moderate yield and traces of other products, which were further characterized by mass spectrometry and no evidence of nitroxide **7a** was found; maybe because the persistence of the spin adducts is very short or because the nitrones are inefficient to trap particular types of radicals as have been reported.¹²

We wish to further explore the reaction mechanism by means of a theoretical model. To this end, we have performed calculations using the Gaussian 98 suit of programs.¹³ To render the calculations tractable, we have reduced the size of the molecule by removing the two phenyl rings, shown here as structure **1'** while the rest of the geometry parameters was taken from the X-ray structure of **2** (Figure 4).

We wish to determine various bond energies of **1'**, in particular, we follow three pathways. The first involves the elimination of the *tert*-butyl group (**2'**) followed by the abstraction of the hydrogen atom H_a (**8'**). In the second pathway the hydrogen atom H_a has been removed (**3'**) which then can either lose also hydrogen atom H_b to form **9'** or lose the *tert*-butyl group as in **8'**. The remaining possibility is the abstraction of hydrogen atom H_b followed by H_a leaving the compound with the *tert*-butyl group **9'**. The three pathway mechanisms are shown in Scheme 2. Note that these are only parts of the mechanism as the newly formed radicals (**6'** and **7'** or **5'** and **7'**) would then go on and form the final products.

Table 3 Reaction of **2** with DMPO

Nitron	Irradiation time (h)	Yield of 3 (%)	Yield of 7a (%)
6a DMPO	75	70.6	–

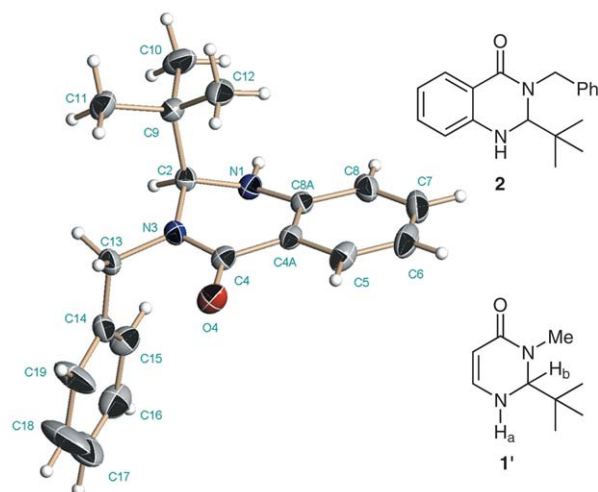


Figure 4 Structures of **2** and **1'**

The energies were determined using the complete basis set method (CBS-4M) to extrapolate the energy missing from incomplete basis set.^{14,15}

The resulting energies are shown in Figure 5. We observed that the third pathway mechanism in which the two hydrogen atoms are removed (via **4'** and **5'**) requires the most energy, with a difference of more than 100 kcal comparing to that of **1'**.

The analogue product of this mechanism was not observed experimentally. The second pathway mechanism (via **3'** and **7'**) leads either to the same high-energy products **9'** and the two hydrogen atoms, or a lower energy product **8'** and hydrogen atom H_a . The energy of this mechanism is lower than the one mentioned above, but it is still almost 10 kcal higher than the first mechanism (via **2'** and **6'**).

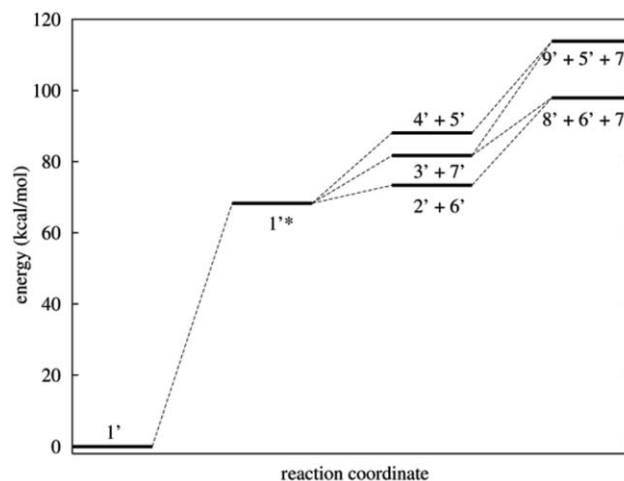
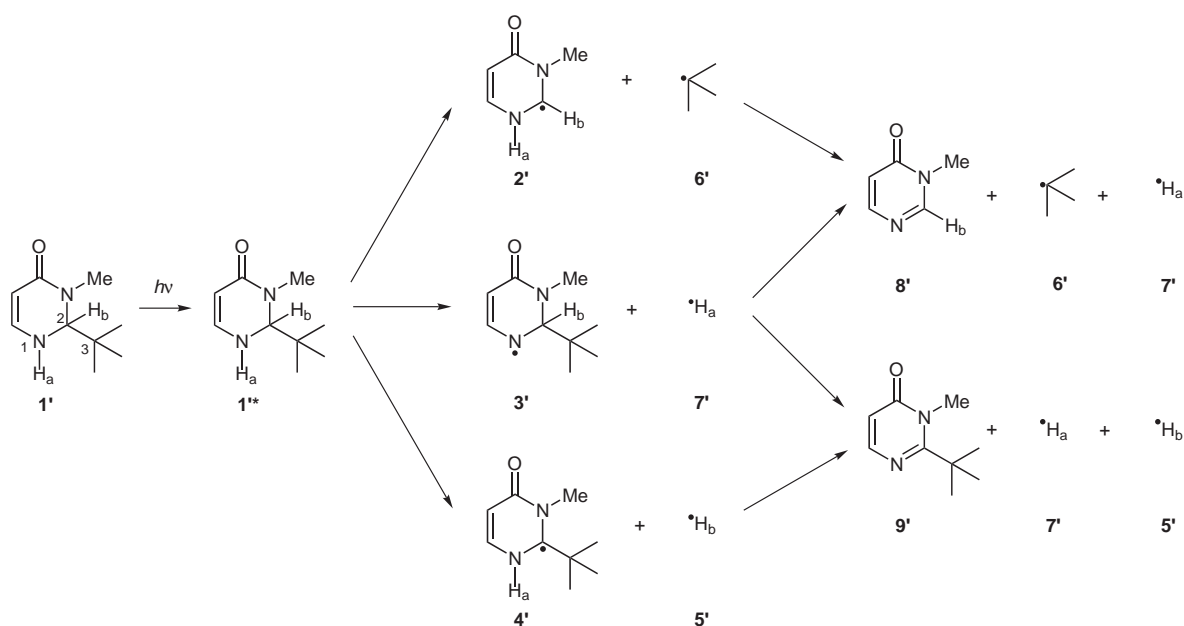


Figure 5 Reaction coordinates of the three (partial) mechanisms

The latter, most energetically favorable of the three, shows a difference of almost 70 kcal for the first step, which could come from the UV radiation and eventually leads to product **8'**, the analogue of which were in fact observed experimentally. The difference in energy in the latter processes, 10 and 30 kcal/mol, respectively, is reasonable within normal experimental conditions.

The nature of the mechanisms can be further explained by studying the electronic properties of the pertinent species. We have performed a topological analysis of the electronic density using the theory of atoms in molecule¹⁶ at the B3LYP/6-311++G** levels. To this end, we have optimized the geometry of **1'** and **2**, which are then characterized by frequency analysis. Since the reaction occurs under radiation, one would suggest that the molecule should first convert into the triplet or singlet excited states before bond breaking could take place. We have therefore



Scheme 2 The three pathway mechanisms

calculated the transition probability to both states using the time-dependent DFT method at the same level of theory B3LYP/6-311++G**. The result shows that the ground state to the triplet transition state is forbidden, while the transition to the first singlet state is possible with the excitation energy of $\lambda = 354.22$ nm. These results are in agreement with experiment evidences. In particular, we observe that the first singlet state involves the excitation of electrons from the S/HOMOs to the LUMO orbital.

The electronic charge density and laplacian of the density at the bond critical points of the N1–H_a, C2–H_b, and C2–C9 bonds of **2**, **1'** and **1'*** were calculated using the PRO-AIM program¹⁷ and tabulated in Table 4. In short, the theory of atoms in molecules states that a chemical bond is characterized by properties at its critical points, in particular, the bond critical point where the gradient of the density vanishes along the trace of the gradient path that connect two atoms.

Table 4 Topological Properties of **2**, our Model **1'**, and the First Singlet State **1'*** from **1'** for the Relevant Bonds

Property	N1–H _a	C2–H _b	C2–C9
ρ (2)	0.16137	0.13269	0.10533
$\nabla^2 \rho$ (2)	–0.03475	0.02148	0.15110
ρ (1')	0.34248	0.28389	0.22638
$\nabla^2 \rho$ (1')	–1.59994	–0.97352	–0.46088
ρ (1'*)	0.34600	0.28610	0.22812
$\nabla^2 \rho$ (1'*)	–1.79885	–1.00997	–0.46496

A negative laplacian indicates a local concentration of electron (normally associated with covalent bond) and a positive laplacian indicates a local depletion of electron which normally characterizes an ionic bonding environment.

We observe in Table 4 that the trend in **1'**, our model, follow well that of compound **2** implying that the removal of the phenyl rings affects the reaction side of the molecule only qualitatively, and therefore, justifies our model. In all three cases, the C2–C9 bond shows the significantly smaller value of density at the bond critical point, showing that it is a weaker bond than the other two.

In the case of the excited singlet state **1'***, the density at the bond critical point of the C2–C9 bond is smaller than the C2–H_b bond and is only two thirds of that of the N1–

H_a bond. Together with the fact that the value of the laplacian is most positive for the C2–C9 bond in all three cases, this bade well for mechanism 1 where the cleavage of the C2–C9 takes place before the two hydrogen atoms. This is not surprising considering the known stability of the *tert*-butyl radical.

In going from the ground state to the excited singlet state, one also notes that there is a displacement of electron away from atoms C2 to the other side of the pyrimidine ring, namely atoms C8A, C4, and C4A (see X-ray structure in Figure 4) while the two hydrogen bonds are essentially unaffected.

This observation is further supported by the HOMO and LUMO diagrams of **1'** shown in Figure 6, where it is noted that there is a (albeit small) bonding contribution to the C2–C9 bond in the HOMO while the LUMO shows a non-bonding contribution at this bond. Furthermore, the LUMO exhibits a building up of electron density in the left half of the ring. Thus, going from the ground state to the excited state brings a small weakening effect to the C2–C9 bond while the H_a and H_b bonds remain unchanged.

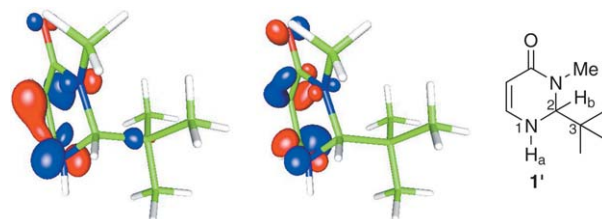
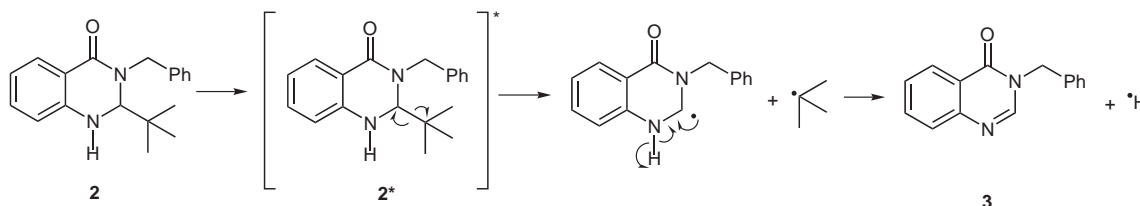


Figure 6 HOMO and LUMO of **1'**. Note the absence of the contribution to the C–C9 bond in the LUMO and in both HOMO and LUMO for N1–H_a and C2–H_b

Thus, theoretical evidences suggest the following mechanism: the UV light irradiation of **2** leads to an excited singlet state **2*** which favors the homolytic rupture of the bond between C2 and the *tert*-butyl group, shown here in step 2 in Scheme 3. In the next step, the newly formed intermediate quinazolinonyl radical loses the hydrogen atom at position N1 to form **3**.

The evolution of the *tert*-butyl radical is worth mentioning since it does raise an interesting question although it does not alter our conclusions. Pryor et al.¹⁸ showed that isobutane, isobutylene, hexamethylethane, etc. are major products derived from the *tert*-butyl radical, while Fischer and collaborators found isobutene produced from the photodissociation of the *tert*-butyl radical.¹⁹ A separate study is

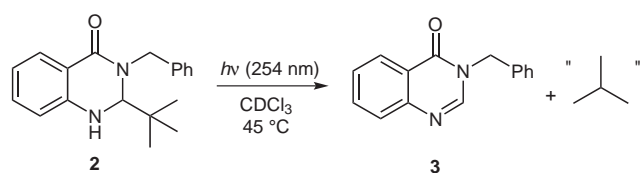


Scheme 3 Proposed mechanism

being conducted in this laboratory, which may shed light on the low yields of the scavenging reactions with TEMPO derivatives.

Finally, Washida and Bayes²⁰ reported that the *tert*-butyl radical can react with an oxygen atom to form the *tert*-butoxy molecule, which then decomposes to form acetone and methyl radicals. The same products are observed when the *tert*-butyl radical reacts with molecular oxygen, albeit with different ratios. To evaluate the role of oxygen, we performed the same reaction with degassed solvent. The results shown in Table 5 suggest that the presence of oxygen accelerates the elimination reaction but does not modify the mechanism in any significant way (Figure 7).

Table 5 Reaction of **2** with Degassed Solvent^a



Time (min)	Degassed proportion 2/3	Normal proportion 2/3
0	100:0	100:0
30	84:16	84:16
60	75:25	70:30
90	63:37	54:46
120	54:46	47:53
150	48:52	35:65
180	42:58	28:72
210	39:61	20:80
240	33:67	18:82 ^c
270	30:70	–
300	24:76 ^b	–

^a [2] = 0.08 M; irradiation time: 30 min (10 mg/0.5 mL).

^b After a drop of D₂O was added the proportion 2/3 was 11:89.

^c After a drop of D₂O was added the proportion 2/3 was 17:83.

In conclusion, we have studied the mechanism of a photoinduced elimination in 2,3-dihydro-2-*tert*-butyl-3-benzyl-4(1*H*)-quinazolinone.²¹ It was found that the reaction was not thermodynamically driven but proceeded only under photochemical conditions, and a free radical mechanism involving abstraction of the *tert*-butyl radical was proposed via theoretical calculations. The presence of the *tert*-butyl radical as intermediate in the reaction was confirmed using different TEMPO derivatives as scavengers. Applications of this methodology to other related 4-quinazolinone derivatives are currently being carried out in our laboratory.

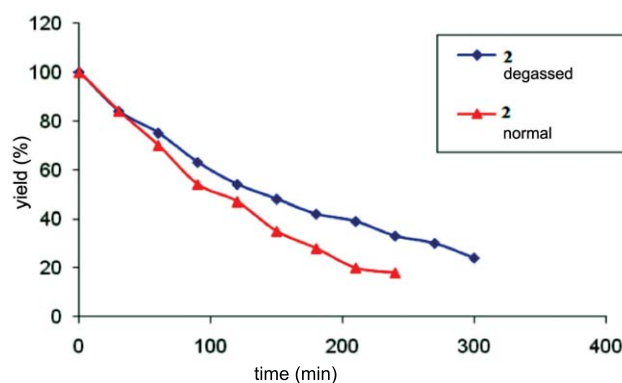


Figure 7 Reaction of **2** with UV radiation ($\lambda = 254$ nm) in degassed and normal solvent

Acknowledgment

We would like to thank Drs. David Crich (Institut de Chimie des Substances Naturelles ICSN, Gif-sur-Yvette, France) and David Rippon (UQUIFA-México) for their suggestions and contributions to use of TEMPO derivatives. We are grateful to CONACYT for financial support (Project No. 48356-Q) and for scholarships to C.O.-N. and F.A.C.-R.; J.M.H.-P. and M.H. acknowledge support from SEP-FORMES2000 for unlimited CPU time on the IBM-p690 32-processor supercomputer at UAEM.

Supporting Information for this article is available online at <http://www.thieme-connect.com/ejournals/toc/synlett>.

References and Notes

- Mhaske, S. B.; Argade, N. P. *Tetrahedron* **2006**, *62*, 9787.
- (a) Larksarp, C.; Alper, H. *J. Org. Chem.* **2000**, *65*, 2773; and references cited therein. (b) Padala, S. R.; Padi, P. R.; Thipireddy, V. *Heterocycles* **2003**, *60*, 183. (c) Maarouf, A. R.; El-Bendary, E. R.; Goda, F. E. *Arch. Pharm. Pharm. Med. Chem.* **2004**, *337*, 527. (d) Xu, Z.; Zhang, Y.; Fu, H.; Zhong, H.; Hong, K.; Zhu, W. *Bioorg. Med. Chem. Lett.* **2011**, *21*, 4005.
- (a) Errede, L. A.; Hill, J. R.; McBrady, J. J. *J. Org. Chem.* **1982**, *47*, 3829. (b) Connolly, D. J.; Cusack, D.; O'Sullivan, T. P. O.; Guiry, P. J. *Tetrahedron* **2005**, *61*, 10153. (c) Leol, Y. C.; Fetting, J. C.; Kurth, M. J. *J. Org. Chem.* **2005**, *70*, 6941. (d) Acharyulu, P. V. R.; Dubey, P. K.; Prasada Reddy, P. V. V.; Suresh, T. *ARKIVOC* **2008**, (xi), 104. (e) Hasegawa, H.; Muraoka, M.; Ohmori, M.; Matsui, K.; Kojima, A. *Bioorg. Med. Chem.* **2005**, *13*, 3721.
- (a) Tangirala, R.; Antony, S.; Agama, K.; Pommier, Y.; Curran, D. P. *Synlett* **2005**, 2843. (b) Bowman, W. R.; Elsegood, M. R. J.; Stein, T.; Weaver, G. W. *Org. Biomol. Chem.* **2007**, *5*, 103.
- Andersin, R.; Mesilaakso, M. *J. Pharm. Biomed. Anal.* **1995**, *13*, 667.
- Nishio, T.; Kameyama, S.; Omote, Y.; Kashima, C. *Heterocycles* **1990**, *30*, 493.
- Kaneko, C.; Kasai, K.; Katagiri, N.; Chiba, T. *Chem. Pharm. Bull.* **1986**, *34*, 3672.
- (a) Escalante, J.; Flores, P.; Priego, J. M. *Heterocycles* **2004**, *63*, 2019. (b) Priego, J.; Flores, P.; Ortiz-Nava, C.; Escalante, J. *Tetrahedron: Asymmetry* **2004**, *15*, 3545. (c) Escalante, J.; Ortiz-Nava, C.; Flores, P.; Priego, J. M.;

- García-Martínez, C. *Molecules* **2007**, *12*, 173. (d) Coppola, G. M. *Synthesis* **1980**, 505.
- (9) Spectral assignments were made with the help of extensive decouplings on authentic samples of the started material **2** and the product **3**.
- (10) (a) Keana, J. F. W. *Chem. Rev.* **1978**, *78*, 37. (b) Vogler, T.; Studer, A. *Synthesis* **2008**, 1979; and references cited therein. (c) Barriga, S. *Synlett* **2001**, 563. (d) Naik, N.; Braslau, R. *Tetrahedron* **1998**, *54*, 667. (e) Calderón, F. *Synlett* **2006**, 657.
- (11) Schoening, K. U.; Fisher, W.; Hauck, S.; Dichtl, A.; Kuepfert, M. *J. Org. Chem.* **2009**, *74*, 1567.
- (12) (a) Villamena, F. A.; Xia, S.; Merle, J. K.; Lauricella, R.; Tuccio, B.; Hadad, C. M.; Zweier, J. L. *J. Am. Chem. Soc.* **2007**, *129*, 8177. (b) Pou, S.; Halpern, H. J.; Tsain, P.; Rosen, G. M. *Acc. Chem. Res.* **1999**, *32*, 155. (c) Villamena, F. A.; Hadad, C. M.; Zweier, J. L. *J. Am. Chem. Soc.* **2004**, *126*, 1816.
- (13) Frisch, M. J.; Trucks, G. W.; Head-Gordon, M.; Gill, P. M. W.; Wong, M. W.; Foresman, J. B.; Johnson, B. G.; Schlegel, H. B.; Robb, M. A.; Repogle, E. S.; Gomperts, R.; Andres, J. L.; Raghavachari, K.; Binkley, J. S.; Gonzalez, C.; Martin, R. L.; Fox, D. J.; DeFrees, D. J.; Baker, J.; Stewart, J. J. P.; Pople, J. A. *GAUSSIAN 98*; Gaussian Inc: Pittsburgh, PA, **1998**.
- (14) (a) Nyden, M. R.; Petersson, G. A. *J. Chem. Phys.* **1981**, *75*, 1843. (b) Petersson, G. A.; Al-Laham, M. A. *J. Chem. Phys.* **1991**, *94*, 6081. (c) Petersson, G. A.; Tensfeldt, T.; Montgomery, J. A. *J. Chem. Phys.* **1991**, *94*, 6091. (d) Montgomery, J. A.; Ochterski, J. W.; Peterson, G. A. *J. Chem. Phys.* **1994**, *101*, 5900.
- (15) (a) Ochterski, J. W.; Petersson, G. A.; Montgomery, J. A.; Pople, J. A. *J. Chem. Phys.* **1996**, *104*, 2598. (b) Curtiss, L. A.; Raghavachari, K.; Redfern, P. C.; Stefanov, B. B. *J. Chem. Phys.* **1998**, *108*, 692.
- (16) Bader, R. F. W. *Atoms in Molecules: A Quantum Theory*; Oxford University Press: Oxford, **1990**.
- (17) PROAIM, obtained from R. F. W. Bader, Department of Chemistry, McMaster University, Hamilton, Ontario, Canada.
- (18) Pryor, W. A.; Tang, F. Y.; Tang, R. H.; Church, D. F. *J. Am. Chem. Soc.* **1982**, *104*, 2885.
- (19) Zierhut, M.; Roth, W.; Fischer, I. *J. Phys. Chem. A* **2004**, *108*, 8125.
- (20) Washida, N.; Bayes, K. D. *J. Phys. Chem.* **1980**, *84*, 1309.
- (21) **Typical Procedure** A solution of **2** (0.34 mmol) in CHCl₃ was stirred and irradiated with UV light in the Rayonet equipment RPR-100. The reaction mixture was monitored by TLC (hexane–EtOAc = 80:20) until the disappearance of the starting material. The reaction mixture was concentrated under reduced pressure, and the crude of the reaction was purified by flash chromatography. When the reaction was examined by ¹H NMR at 400 MHz, peak ratios were determined by integration of the spectrum with an estimated error of ca. 5%.

Copyright of Synlett is the property of Georg Thieme Verlag Stuttgart and its content may not be copied or emailed to multiple sites or posted to a listserv without the copyright holder's express written permission. However, users may print, download, or email articles for individual use.